Supplement of Weather Clim. Dynam., 5, 895–912, 2024
https://doi.org/10.5194/wcd-5-895-2024-supplement

Supplement of

Large-ensemble assessment of the Arctic stratospheric polar vortex morphology and disruptions

Ales Kuchar et al.

Correspondence to: Ales Kuchar (ales.kuchar@boku.ac.at)

S1 Table of concents

- Tables S1 and S2
- ROC curves for displacement and split events (Figs. S1 and S2)
- Rank Histograms for 50 hPa and 100 hPa (Figs. S3-S12)

S2 Moment diagnostics of the polar vortex

The first step of the calculation is to define the limit of the vortex. The vortex is described by the area that has lower values of geopotential height than the limit, values higher than the limit are set equal to the limit so that these values do not contribute to the calculation of the diagnostics.

For the moment calculations (Eq. 3), the coordinates from the output of the climate models have to be converted from spherical to Cartesian ones. This is done by using Lambert's azimuthal equal-area projection, which converts a coordinate of latitude ϕ and longitude λ to Cartesian Coordinates x and y, while preserving the area of the vortex:

$$\begin{aligned} x &= R\cos\lambda \\ y &= R\sin\lambda \end{aligned} \tag{1}$$

with

$$R = a\sqrt{2(1-\sin\phi)} \tag{2}$$

and the Earth's radius $a = 6374\,\mathrm{km}$.

The absolute vortex moment is defined as:

$$M_{kl} = \int\int (q-q_b)x^k y^l \mathrm{d}x\mathrm{d}y \tag{3}$$

where q is the actual geopotential height, after values higher than the limit have been truncated, and q_b is the value of the limit. The integration is carried out by summing over each grid point available in the model output. The moment is two-dimensional so two separate exponents are necessary: k for the x-direction and l for the y-direction.

Using the absolute vortex moment, we can determine the center of the vortex (centroid) in Cartesian coordinates:

$$(\bar{x},\bar{y}) = \frac{(M_{10}, M_{01})}{M_{00}} \tag{4}$$

With the help of the centroid coordinates, we can calculate the relative vortex moment:

$$J_{kl} = \int\int (q-q_b)(x-\bar{x})^k (y-\bar{y})^l \mathrm{d}x\mathrm{d}y \tag{5}$$

which is needed to retrieve the moment diagnostics describing different characteristics of the polar vortex, which will be explained in the following

S2.1 Angle

The angle ψ describes the orientation of the polar vortex. To this end, the vortex is represented by an ellipse and ψ is the angle between its major axis and the x-axis, which lies on the meridian of 90°W and 90°E because of the conversion from spherical to Cartesian coordinates.

$$\psi = \frac{1}{2}\tan^{-1}\left(\frac{J_{11}}{J_{20}-J_{02}}\right) \tag{6}$$

S2.2 Aspect ratio

The aspect ratio of the ellipse is the ratio of its major axis to its minor axis. This diagnostic describes how stretched the vortex is: A higher value indicates a strongly stretched vortex, whereas a lower aspect ratio implies a more circular polar vortex. An exceptionally high value is often associated with a disturbance of the polar vortex.

$$r = \left| \frac{(J_{20}+J_{02}) + \sqrt{4J_{11}^2 + (J_{20}-J_{02})}}{(J_{20}+J_{02}) + \sqrt{4J_{11}^2 + (J_{20}-J_{02})}} \right|^{\frac{1}{2}} \tag{7}$$

S2.3 Objective area

The area of the ellipse is an indicator of the strength of the polar vortex.

$$A = \frac{M_{00}}{q_b} \tag{8}$$

S2.4 Kurtosis

The excess kurtosis reveals how the values of geopotential height are distributed within the ellipse describing the polar vortex. An excess kurtosis of 0 is reached, if the value of geopotential height is constant. Negative values are achieved when two separate areas of low geopotential height exist, e.g. when the vortex splits. High values are produced when the geopotential height in the center is low and has higher values surrounding it.

S2.5 Centroid Latitude and Centroid Longitude

The location of the centroid of the polar vortex in Cartesian Coordinates (Eq. 4) can be transferred back to spherical coordinates, which gives us the centroid latitude and centroid longitude. This simplifies the interpretation of the centroid coordinates, e.g. a lower centroid latitude is often associated with a disrupted vortex and can be indicative of a displacement.

S3 ROC curves

The receiver operating characteristic (ROC) curves are plotted in a diagram with the false positive rate on the x-axis and the true positive rate on the y-axis (see Figs. S1 and S2). In this specific case, the false positive rate indicates the probability that the ensemble is simulating an event, even though there was no event observed in the reanalysis. The true positive rate is the probability that the ensemble detects an event when it actually occurs. For an ideal forecast, the curve goes along the y-axis at a false positive rate of 0 and when it reaches the top of the diagram, it moves in the x-direction to the right side of the diagram. An ensemble that produces a curve that describes the diagonal line in the plot is not better than randomly guessing the occurrence of the events. To make the interpretation easier the area under the ROC curve (AOC) can be calculated. In an ideal case, the area is equal to 1. For the case where the curve coincides with the diagonal, the area is equal to 0.5. For further details about the application and interpretation of the ROC diagram we refer to Wilks (2011) or Jolliffe and Stephenson (2012).

S4 Tables

Table S1: Summary table including metrics: bias, spread and AOC. AOC related to displacement and split events is in the table associated with centroid latitude and aspect ratio, respectively.

		100 hPa			50 hPa			10 hPa		
		bias	spread	AUC	bias	spread	AUC	bias	spread	AUC
CanESM2	aspect ratio	590.99	213.27		210.74	54.06		148.61	7.10	0.55
	objective area	343.13	122.48		15.73	77.34		197.27	128.91	
	kurtosis	11.78	226.71		591.70	240.18		**5525.35**	3790.66	
	centroid latitude	418.52	79.54		336.71	53.66		781.14	47.83	0.66
	centroid longitude	118.84	66.86		3.13	141.43		224.01	13.95	
CanESM5	aspect ratio	184.78	48.57		266.95	59.42		772.06	140.74	**0.45**
	objective area	894.65	1.51		**1520.33**	23.75		425.06	11.87	
	kurtosis	118.64	411.00		16.80	353.75		4577.71	**4368.73**	
	centroid latitude	290.00	53.74		276.07	65.13		19.30	6.20	0.59
	centroid longitude	44.20	47.26		1.48	15.65		120.33	224.55	
CESM2	aspect ratio	104.88	10.34		271.81	32.92		576.90	127.07	0.59
	objective area	334.06	91.54		476.74	166.81		1587.79	344.51	
	kurtosis	6.82	217.62		61.09	378.66		2239.48	2203.39	
	centroid latitude	252.67	88.90		366.22	115.06		233.96	21.51	0.61
	centroid longitude	26.31	50.33		**0.01**	33.15		67.85	56.46	
CNRM-CM6-1	aspect ratio	6.74	0.72		14.67	**0.03**		108.77	0.28	0.64
	objective area	3.00	5.46		51.57	14.76		847.55	78.80	
	kurtosis	227.27	10.95		866.92	176.20		4018.98	2329.24	
	centroid latitude	**0.06**	2.24		22.69	0.35		15.46	8.79	**0.71**
	centroid longitude	0.39	4.15		15.80	2.72		0.90	2.94	
INM-CM5-0	aspect ratio	257.00	69.24		119.68	51.19		0.65	1.80	0.53
	objective area	26.65	71.31		71.70	80.82		165.95	436.67	
	kurtosis	52.26	221.07		114.18	133.80		3.01	25.45	
	centroid latitude	304.27	182.85		391.94	148.44		90.28	7.54	0.67
	centroid longitude	55.00	53.04		0.03	75.01		0.52	7.36	
IPSL-CM6A-LR	aspect ratio	41.73	4.27		115.30	15.54		450.04	2.55	0.63
	objective area	507.80	75.51		137.37	71.86		570.49	730.88	
	kurtosis	1.26	94.65		10.65	132.02		45.86	69.42	
	centroid latitude	44.41	18.49		64.22	46.14		156.46	7.66	0.63
	centroid longitude	77.08	41.45		3.29	403.83		289.33	6.17	
MIROC6	aspect ratio	8.38	7.86		6.06	13.84		19.07	6.55	0.59
	objective area	841.65	420.28		900.00	**790.83**		624.89	1015.18	
	kurtosis	62.65	0.38		19.48	15.54		40.58	19.20	
	centroid latitude	0.16	19.33		97.24	43.67		332.99	19.25	0.62
	centroid longitude	101.61	9.90		26.33	199.91		209.12	4.14	
UKESM1-0-LL	aspect ratio	99.95	19.77		91.16	17.09		**0.33**	0.27	0.58
	objective area	0.15	127.42		161.29	91.84		67.10	14.83	

Continued on next page

Table S1: Summary table including metrics: bias, spread and AOC. AOC related to displacement and split events is in the table associated with centroid latitude and aspect ratio, respectively. We mark the model with the best and worst performance by red and blue color, respectively.

		100 hPa			50 hPa			10 hPa		
		bias	spread	AUC	bias	spread	AUC	bias	spread	AUC
	kurtosis	54.18	107.00		17.97	51.80		421.63	99.53	
	centroid latitude	1.94	**0.19**		18.81	1.03		16.88	27.50	0.66
	centroid longitude	0.33	5.42		1.19	3.25		156.71	29.47	
MPI-ESM1-2-HR	aspect ratio	1.81	2.84		11.33	1.06		116.15	**0.01**	0.56
	objective area	535.27	72.35		484.98	196.42		1046.07	824.85	
	kurtosis	3.57	8.82		27.34	78.91		453.43	40.79	
	centroid latitude	151.91	10.35		89.40	7.42		123.33	0.91	0.59
	centroid longitude	16.50	9.09		1.26	13.32		4.53	80.94	
MPI-ESM1-2-LR	aspect ratio	3.77	0.56		11.93	0.55		242.95	7.78	0.65
	objective area	1030.16	372.84		776.32	568.10		1118.40	1266.02	
	kurtosis	1.91	13.73		0.04	71.31		324.23	102.14	
	centroid latitude	298.72	32.05		154.32	12.51		199.48	21.33	0.66
	centroid longitude	0.65	57.89		26.56	2.04		39.20	214.11	
GFDL-CM3	aspect ratio	271.25	116.71							
	objective area	**6615.54**	**2364.37**							
	kurtosis	42.21	423.25							
	centroid latitude	471.85	282.04							
	centroid longitude	69.90	52.72							

Table S2. List of SSWs in ERA5

	onset dates	vortex type
0	1979-02-22	split
1	1980-02-29	displaced
2	1981-03-04	displaced
3	1981-12-04	unclassified
4	1984-02-23	displaced
5	1985-01-01	split
6	1987-01-23	displaced
7	1987-12-08	split
8	1988-03-14	split
9	1989-02-21	split
10	1998-12-15	displaced
11	1999-02-25	split
12	2000-03-20	displaced
13	2001-02-11	split
14	2001-12-30	displaced
15	2002-02-17	displaced
16	2003-01-18	split
17	2004-01-05	displaced
18	2006-01-21	displaced
19	2007-02-24	displaced
20	2008-02-22	displaced
21	2009-01-24	split
22	2010-02-09	displaced
23	2010-03-24	displaced
24	2013-01-06	split

S5 Figures

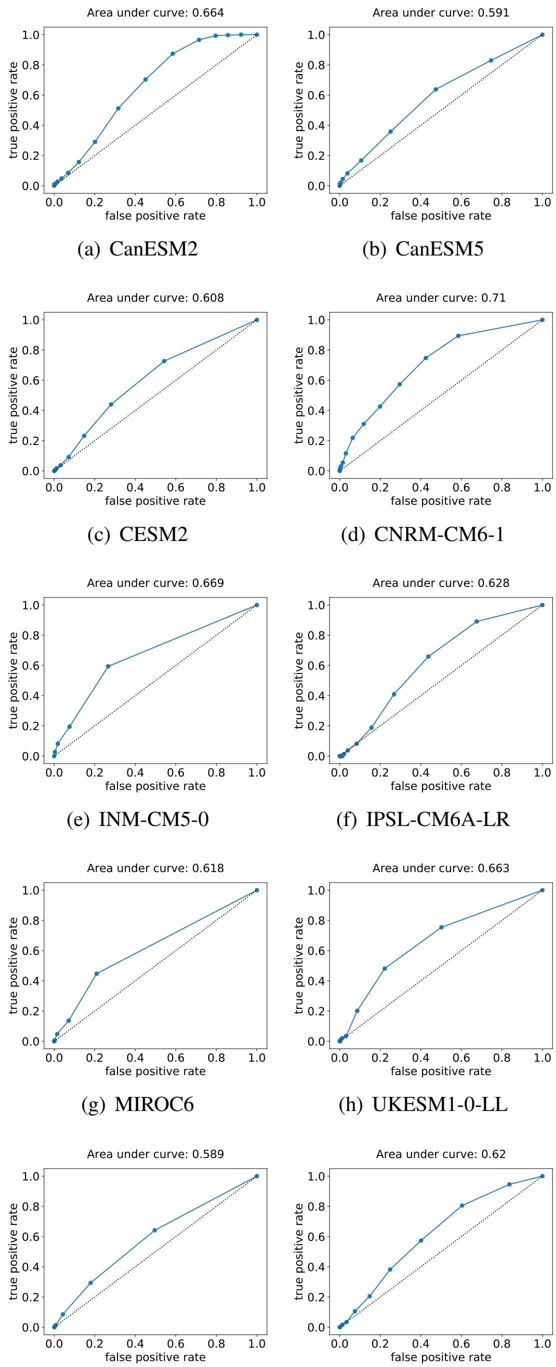

(a) CanESM2 (b) CanESM5

(c) CESM2 (d) CNRM-CM6-1

(e) INM-CM5-0 (f) IPSL-CM6A-LR

(g) MIROC6 (h) UKESM1-0-LL

(i) MPI-ESM1-2-HR (j) MPI-ESM1-2-LR

Figure S1. ROC curves for displacement events

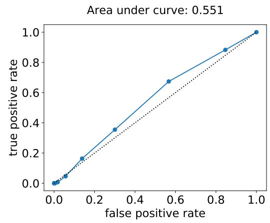

(a) CanESM2

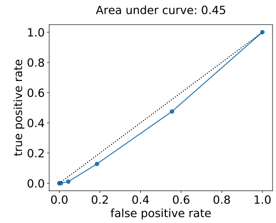

(b) CanESM5

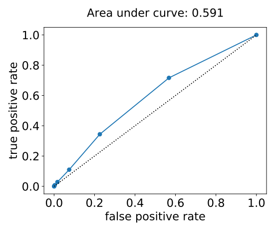

(c) CESM2

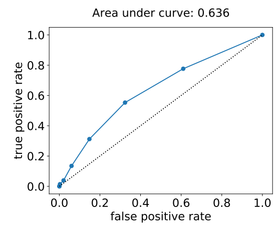

(d) CNRM-CM6-1

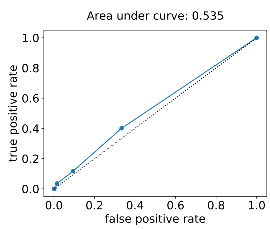

(e) INM-CM5-0

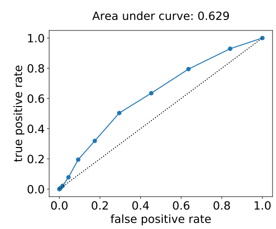

(f) IPSL-CM6A-LR

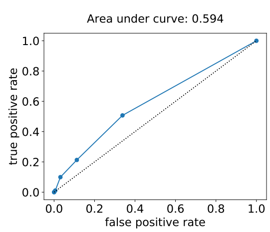

(g) MIROC6

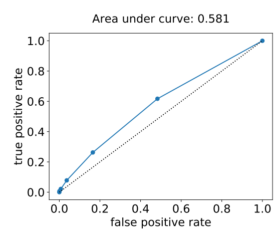

(h) UKESM1-0-LL

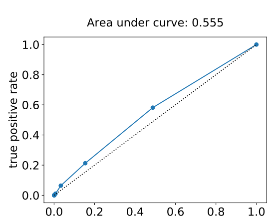

(i) MPI-ESM1-2-HR

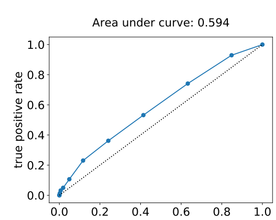

(j) MPI-ESM1-2-LR

Figure S2. ROC curves for split events

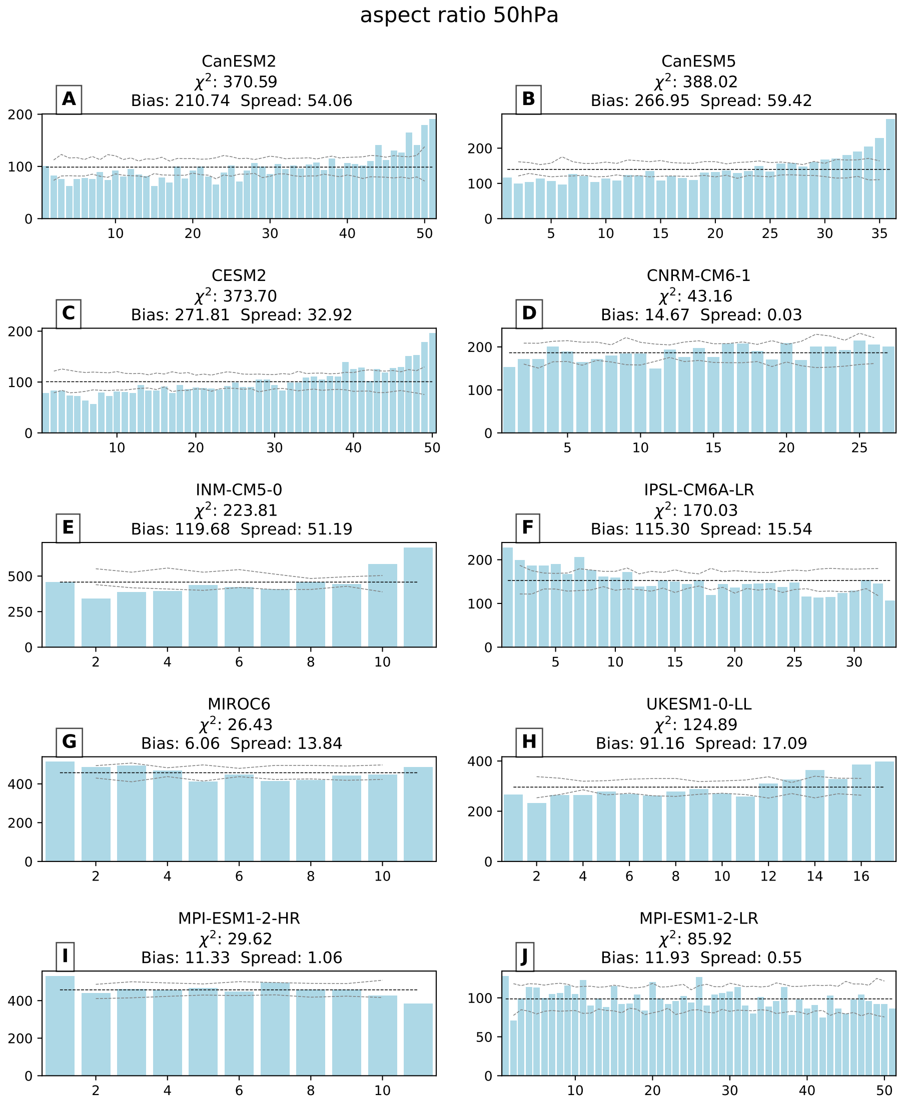

Figure S3. Rank histograms of aspect ratio at 50 hPa of all analyzed model ensembles: CanESM2 (**A**), CanESM5 (**B**), CESM2 (**C**), CNRM-CM6-1 (**D**), INM-CM5-0 (**E**), IPSL-CM6A-LR (**F**), MIROC6 (**G**), UKESM1-0-LL (**H**), MPI-ESM1-2-HR (**I**) and MPI-ESM1-2-LR (**J**) with their respective statistics. Blue bars show counts for the individual bins, the black dashed line corresponds to the expected value for a flat histogram, the grey dashed lines indicate the perfect model range.

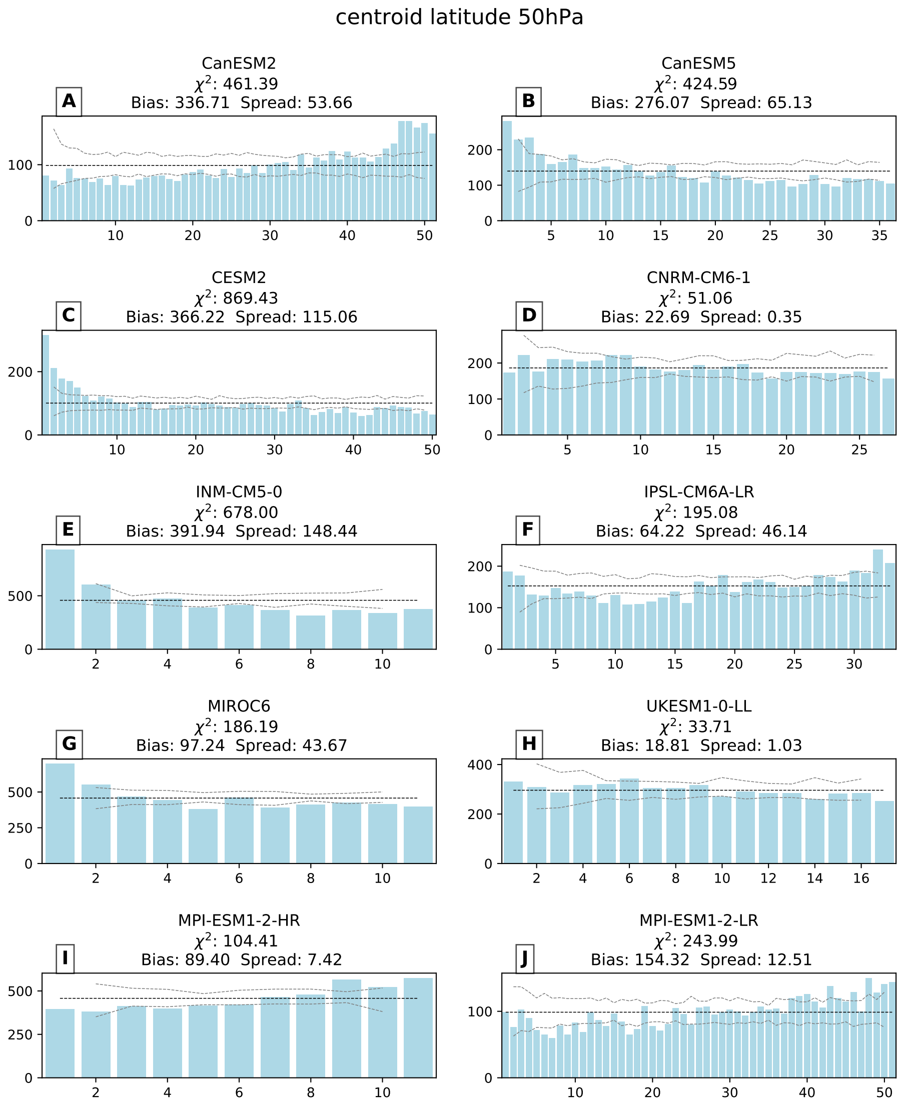

Figure S4. As figure S3 but for centroid latitude at 50 hPa of all analyzed model ensembles: CanESM2 (**A**), CanESM5 (**B**), CESM2 (**C**), CNRM-CM6-1 (**D**), INM-CM5-0 (**E**), IPSL-CM6A-LR (**F**), MIROC6 (**G**), UKESM1-0-LL (**H**), MPI-ESM1-2-HR (**I**) and MPI-ESM1-2-LR (**J**).

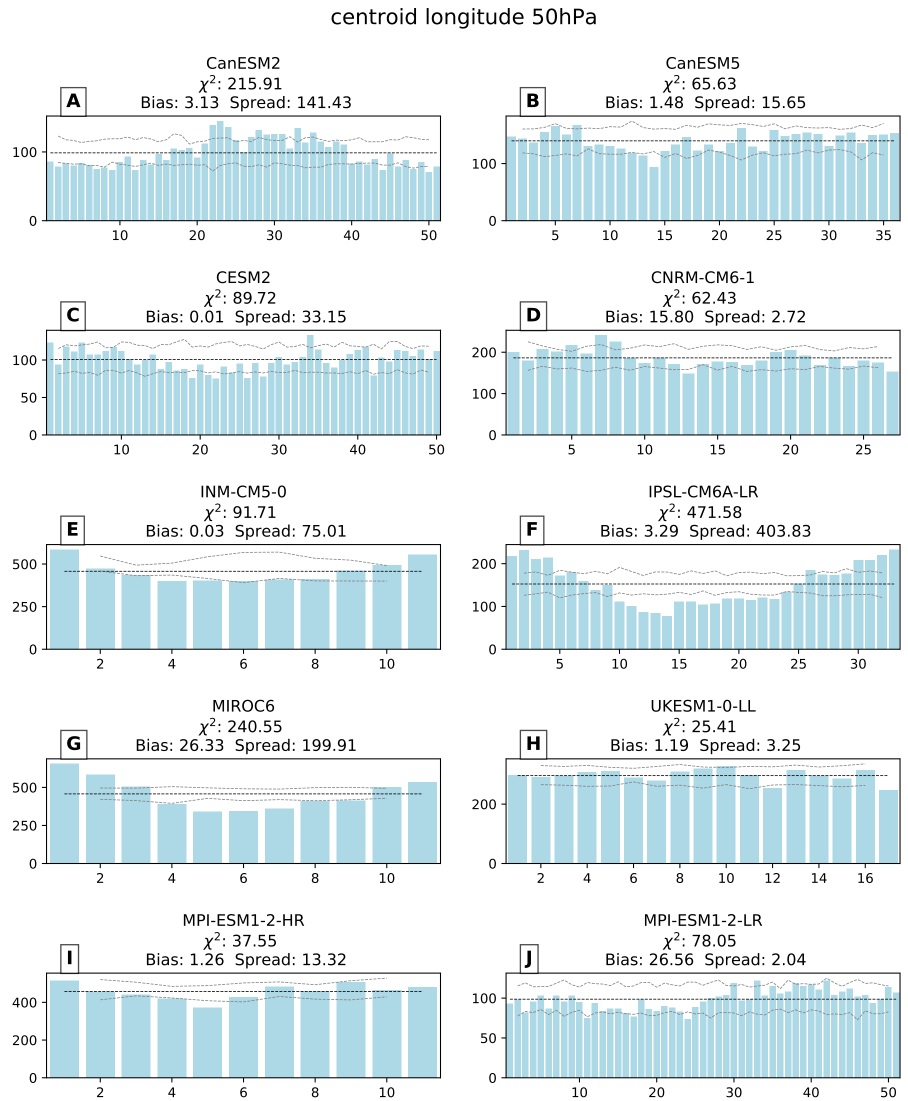

Figure S5. As figure S3 but for centroid longitude at 50 hPa of all analyzed model ensembles: CanESM2 (**A**), CanESM5 (**B**), CESM2 (**C**), CNRM-CM6-1 (**D**), INM-CM5-0 (**E**), IPSL-CM6A-LR (**F**), MIROC6 (**G**), UKESM1-0-LL (**H**), MPI-ESM1-2-HR (**I**) and MPI-ESM1-2-LR (**J**).

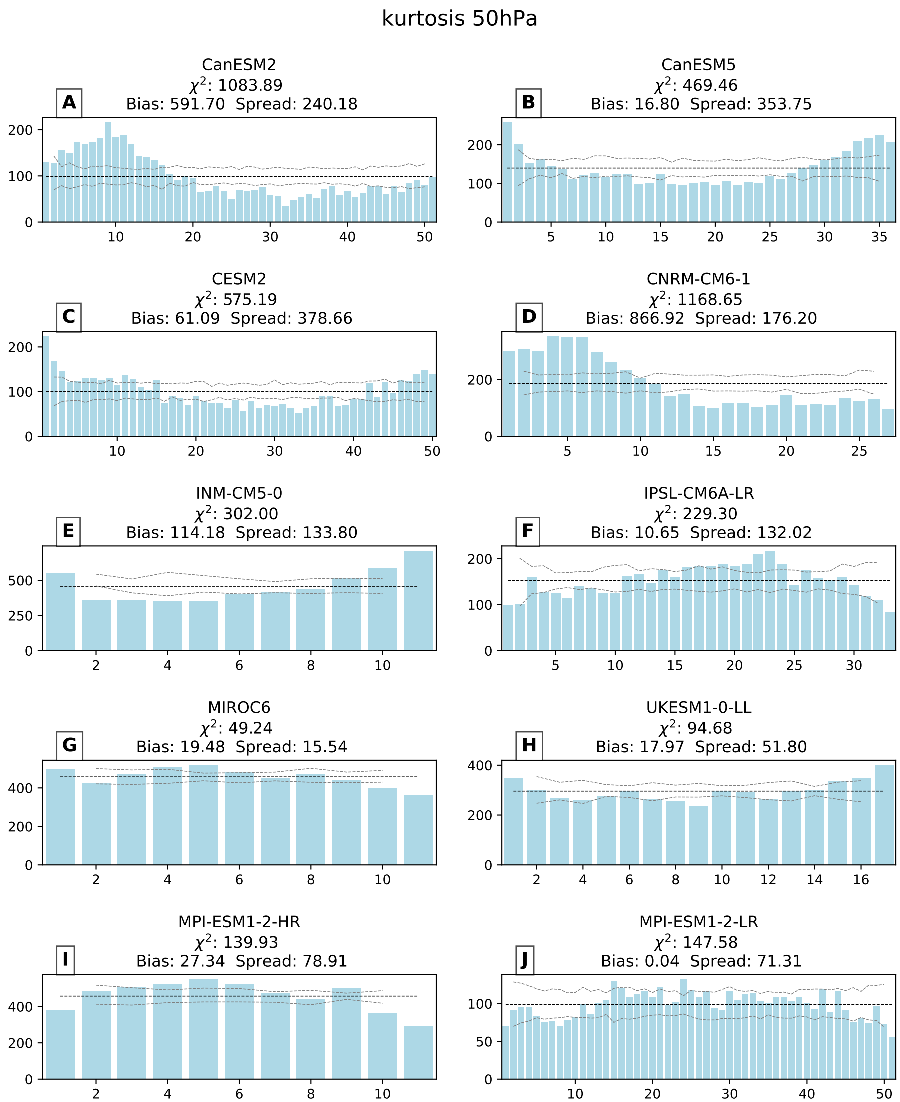

Figure S6. As figure S3 but for kurtosis at 50 hPa of all analyzed model ensembles: CanESM2 (**A**), CanESM5 (**B**), CESM2 (**C**), CNRM-CM6-1 (**D**), INM-CM5-0 (**E**), IPSL-CM6A-LR (**F**), MIROC6 (**G**), UKESM1-0-LL (**H**), MPI-ESM1-2-HR (**I**) and MPI-ESM1-2-LR (**J**).

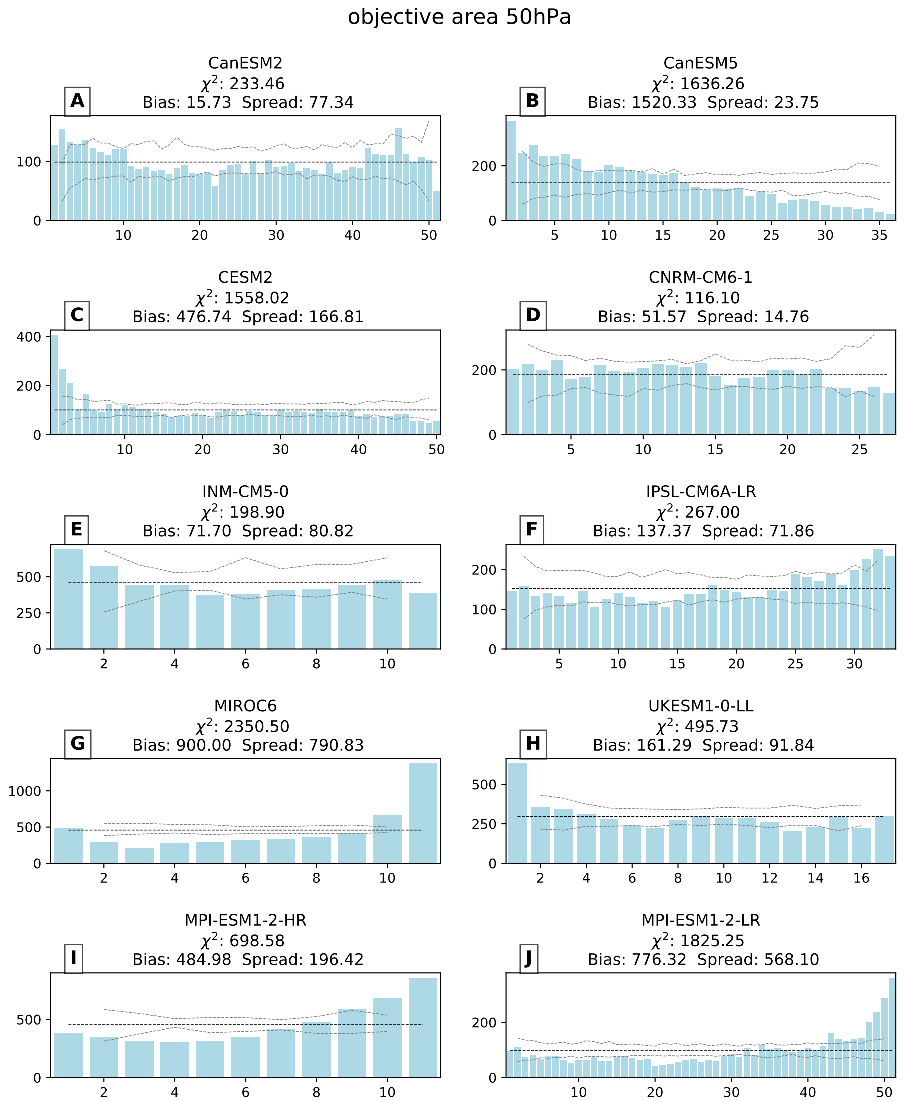

Figure S7. As figure S3 but for objective area at 50 hPa of all analyzed model ensembles: CanESM2 (**A**), CanESM5 (**B**), CESM2 (**C**), CNRM-CM6-1 (**D**), INM-CM5-0 (**E**), IPSL-CM6A-LR (**F**), MIROC6 (**G**), UKESM1-0-LL (**H**), MPI-ESM1-2-HR (**I**) and MPI-ESM1-2-LR (**J**).

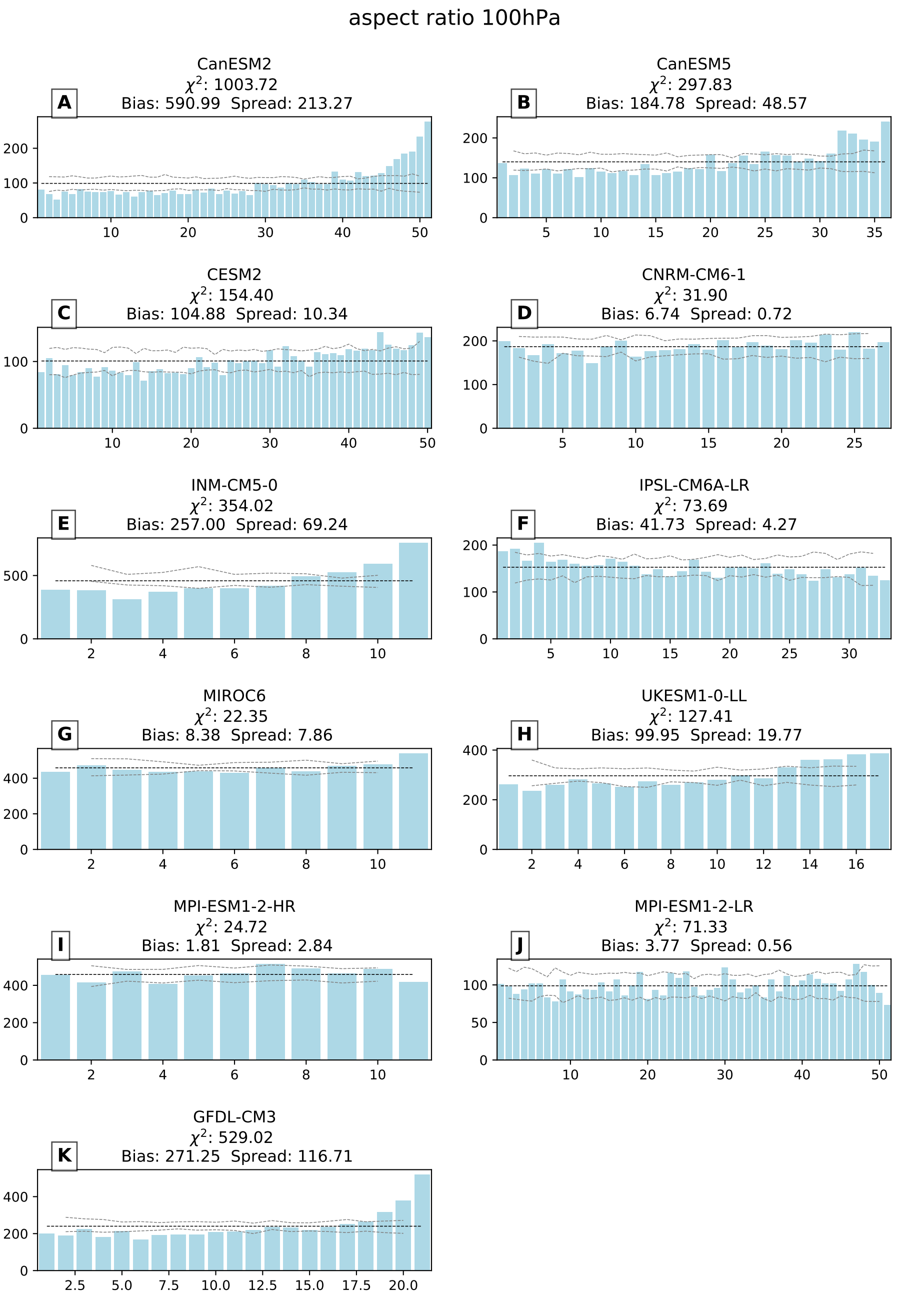

Figure S8. As figure S3 but for aspect ratio at 100 hPa of all analyzed model ensembles: CanESM2 (**A**), CanESM5 (**B**), CESM2 (**C**), CNRM-CM6-1 (**D**), INM-CM5-0 (**E**), IPSL-CM6A-LR (**F**), MIROC6 (**G**), UKESM1-0-LL (**H**), MPI-ESM1-2-HR (**I**), MPI-ESM1-2-LR (**J**) and GFDL-CM3 (**K**).

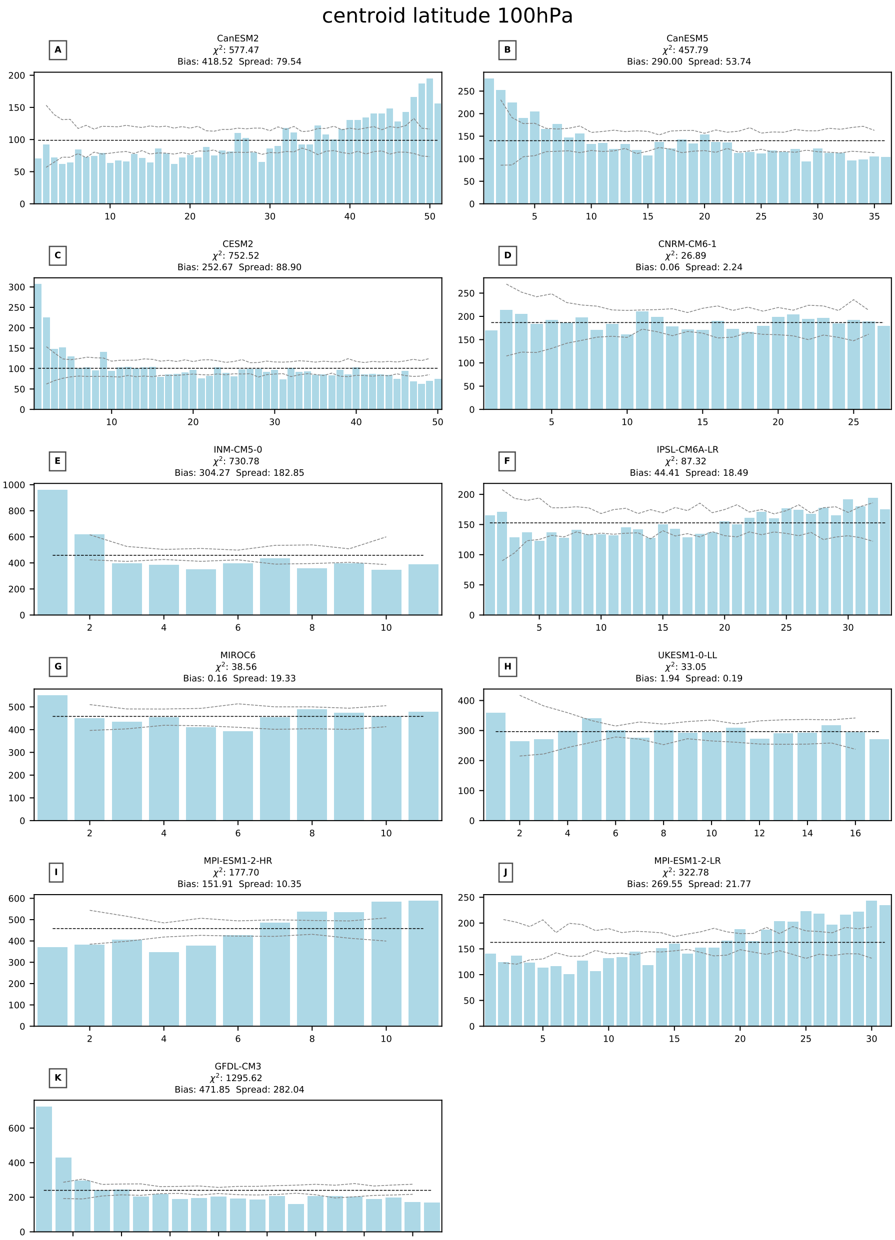

Figure S9. As figure S3 but for centroid latitude at 100 hPa of all analyzed model ensembles: CanESM2 (**A**), CanESM5 (**B**), CESM2 (**C**), CNRM-CM6-1 (**D**), INM-CM5-0 (**E**), IPSL-CM6A-LR (**F**), MIROC6 (**G**), UKESM1-0-LL (**H**), MPI-ESM1-2-HR (**I**), MPI-ESM1-2-LR (**J**) and GFDL-CM3 (**K**).

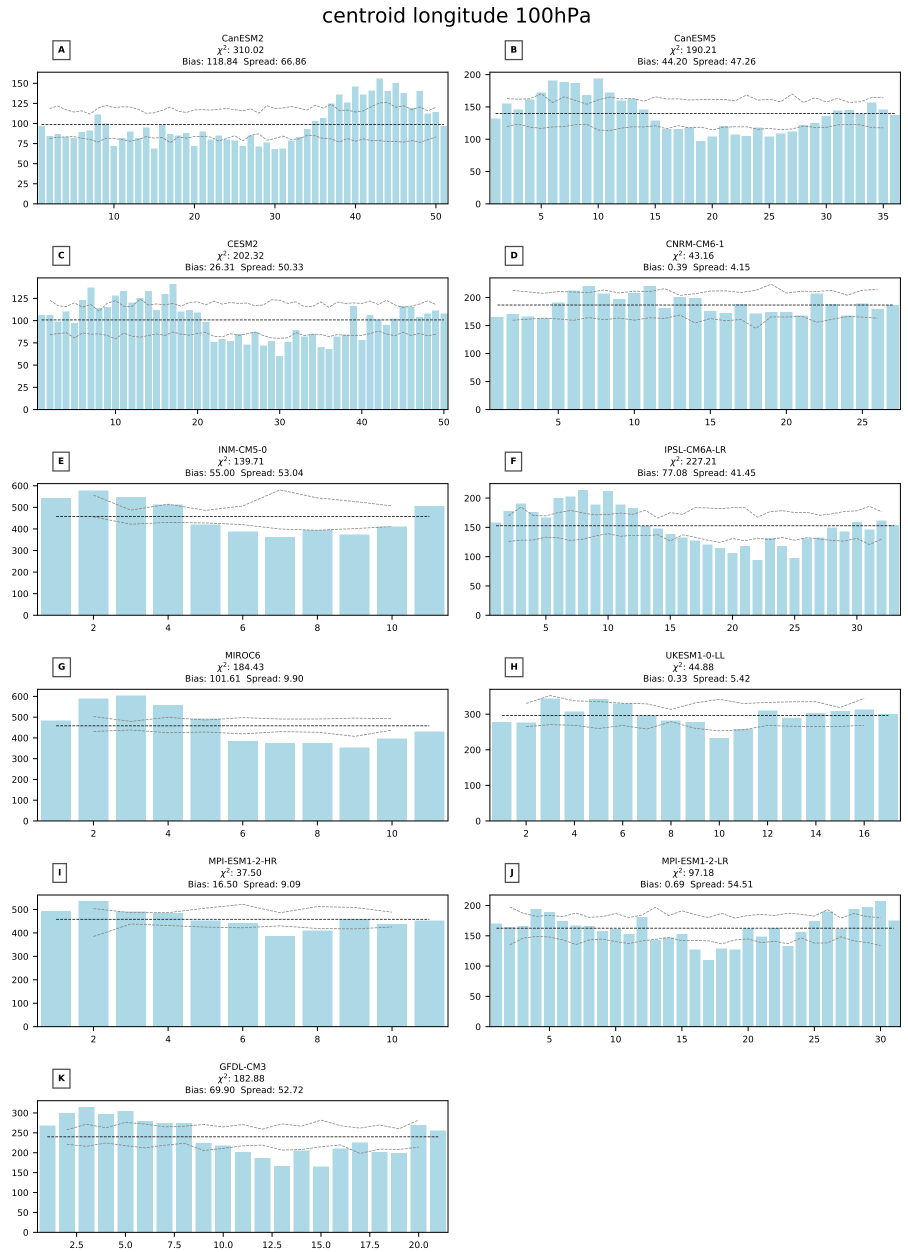

Figure S10. As figure S3 but for centroid longitude at 100 hPa of all analyzed model ensembles: CanESM2 (**A**), CanESM5 (**B**), CESM2 (**C**), CNRM-CM6-1 (**D**), INM-CM5-0 (**E**), IPSL-CM6A-LR (**F**), MIROC6 (**G**), UKESM1-0-LL (**H**), MPI-ESM1-2-HR (**I**), MPI-ESM1-2-LR (**J**) and GFDL-CM3 (**K**).

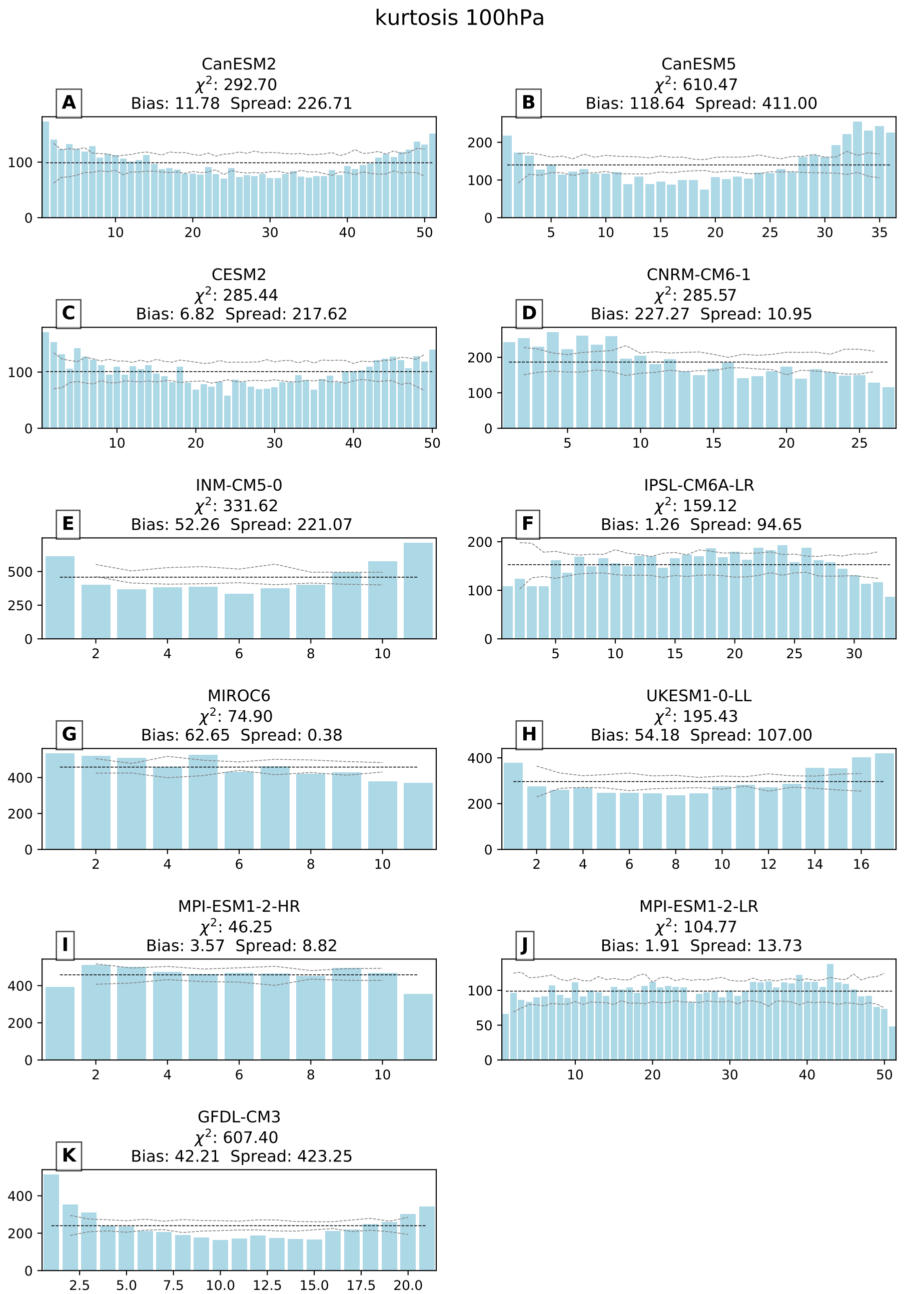

Figure S11. As figure S3 but for kurtosis at 100 hPa of all analyzed model ensembles: CanESM2 (**A**), CanESM5 (**B**), CESM2 (**C**), CNRM-CM6-1 (**D**), INM-CM5-0 (**E**), IPSL-CM6A-LR (**F**), MIROC6 (**G**), UKESM1-0-LL (**H**), MPI-ESM1-2-HR (**I**), MPI-ESM1-2-LR (**J**) and GFDL-CM3 (**K**).

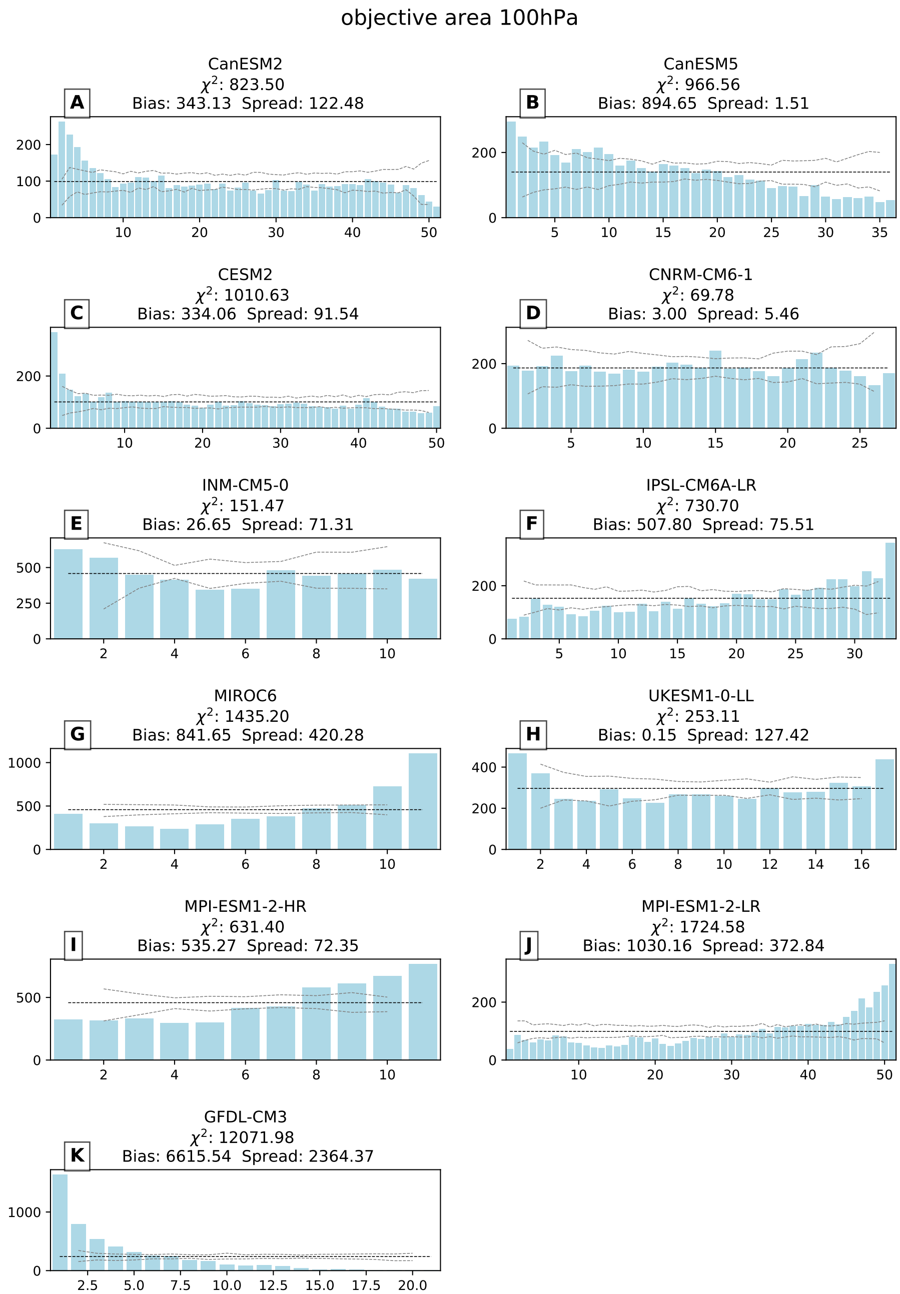

Figure S12. As figure S3 but for objective area at 100 hPa of all analyzed model ensembles: CanESM2 (**A**), CanESM5 (**B**), CESM2 (**C**), CNRM-CM6-1 (**D**), INM-CM5-0 (**E**), IPSL-CM6A-LR (**F**), MIROC6 (**G**), UKESM1-0-LL (**H**), MPI-ESM1-2-HR (**I**), MPI-ESM1-2-LR (**J**) and GFDL-CM3 (**K**).

References

Jolliffe, I. T. and Stephenson, D. B.: Forecast verification: a practitioner's guide in atmospheric science, John Wiley & Sons, 2012.
Wilks, D. S.: Statistical methods in the atmospheric sciences, vol. 100, Academic press, 2011.